International Journal of Scientific Research and Engineering Development-– Volume 8 Issue 5, Sep-Oct 2025
Available at www.ijsred.com

RESEARCH ARTICLE OPEN ACCESS

Micromagnetic Simulation: Methods, Applications, and Recent Advances

Shidas Kalappadan

Abstract:

Micromagnetics is the continuum theory of magnetization dynamics at sub-micrometer length scales and nanosecond time scales. It forms the computational backbone for modelling domain structures, magnetization switching, spin-transfer and spin-orbit torques, and emergent topological magnetic textures such as skyrmions. This paper presents a comprehensive treatment of the micromagnetic model, numerical techniques used in simulations, commonly used software, representative case studies (domain-wall dynamics, skyrmion motion, magnetization reversal), and recent advances including multiscale coupling and GPU acceleration. Important numerical considerations, benchmarking strategies, and open challenges are discussed. The provided LaTeX source is intended as a standalone, publication-ready draft and includes placeholders for figures and extended references.

1 Introduction

Micromagnetics is the continuum description of magnetization in ferromagnetic materials where the magnetization $\mathbf{M}(\mathbf{r},t)$ varies slowly on the scale of the atomic lattice but can develop complex mesoscale structures such as domain walls and vortices. The theory sits between atomistic spin models and macroscopic phenomenology, capturing exchange interactions, magnetocrystalline anisotropy, magnetostatic effects, and interactions with external fields and currents. Computational micromagnetics has become essential in the design and understanding of modern spintronic devices, magnetic memory (MRAM), and nanomagnetic logic.

The goal of this paper is to present a self-contained review of the micromagnetic framework and computational approaches, to describe typical case studies, and to highlight current technical advances and challenges. The structure is as follows: Section 2 reviews the governing equations and energy terms. Section 3 discusses numerical methods and stability considerations. Section 4 surveys popular simulation packages. Section 5 presents three representative case studies. Section 6 addresses recent directions, and Section 8 lists open problems and future opportunities. Finally, conclusions are presented in Section **??**.

2 Fundamentals of Micromagnetics

In micromagnetics the state variable is the magnetization field $\mathbf{M}(\mathbf{r},t)$ with magnitude M_s (saturation magnetization). It is customary to work with the normalized magnetization $\mathbf{m}(\mathbf{r},t) = \mathbf{M}/M_s$ such that $|\mathbf{m}| = 1$.

2.1 Energy Functional

The total micromagnetic energy $E[\mathbf{m}]$ is the integral over volume of various energy density contributions:

$$E = \int_V (\varepsilon_{\text{ex}} + \varepsilon_{\text{ani}} + \varepsilon_{\text{ms}} + \varepsilon_{\text{Z}} + \varepsilon_{\text{DMI}})\, dV, \tag{1}$$

where the common terms are:

Exchange energy

$$\varepsilon_{\text{ex}} = A\,(\nabla \mathbf{m})^2 = A \sum_{i=1}^{3} \sum_{j=1}^{3} \left(\frac{\partial m_i}{\partial x_j} \right)^2, \tag{2}$$

with exchange stiffness A (J/m). Exchange favors uniform magnetization.

Anisotropy energy For uniaxial anisotropy with easy axis $\mathbf{e}_u$ and constant K_u:

$$\varepsilon_{\text{ani}} = K_u \left(1 - (\mathbf{m} \cdot \mathbf{e}_u)^2\right). \tag{3}$$

Magnetostatic (demagnetizing) energy

$$\varepsilon_{\text{ms}} = -\frac{\mu_0}{2} \mathbf{M} \cdot \mathbf{H}_d, \tag{4}$$

where $\mathbf{H}_d$ is the demagnetizing field, solution of

$$\nabla \cdot (\mathbf{H}_d + \mathbf{M}) = 0, \qquad \nabla \times \mathbf{H}_d = 0. \tag{5}$$

Equivalently, $\mathbf{H}_d = -\nabla U$ with magnetostatic potential U determined by Poissonlike equations and surface/volume magnetic charges.

Zeeman energy In an external applied field $\mathbf{H}_{\text{ext}}$:

$$\varepsilon_Z = -\mu_0 \mathbf{M} \cdot \mathbf{H}_{\text{ext}}. \tag{6}$$

Dzyaloshinskii–Moriya interaction (DMI) In systems with broken inversion symmetry (interfaces or non-centrosymmetric crystals) an interfacial or bulk DMI contributes:

$$\varepsilon_{\text{DMI}} = D\mathbf{m} \cdot (\nabla \times \mathbf{m}) \qquad (\textit{bulkform, orinterfacialvariants}). \tag{7}$$

DMI stabilizes chiral textures such as N´eel-type walls and skyrmions.

2.2 Effective Field and Dynamics

The effective field $\mathbf{H}_{\text{eff}}$ is defined variationally:

$$\mathbf{H}_{\text{eff}} = -\frac{1}{\mu_0 M_s} \frac{\delta E}{\delta \mathbf{m}}. \tag{8}$$

Magnetization dynamics are governed by the Landau–Lifshitz–Gilbert (LLG) equation:

$$\frac{\partial \mathbf{m}}{\partial t} = -\gamma\, \mathbf{m} \times \mathbf{H}_{\text{eff}} + \alpha\, \mathbf{m} \times \frac{\partial \mathbf{m}}{\partial t}, \tag{9}$$

where γ is the gyromagnetic ratio (rad s^{-1} T^{-1}) and α is the dimensionless Gilbert damping parameter. Rearranging,

$$(1 + \alpha^2) \frac{\partial \mathbf{m}}{\partial t} = -\gamma \mathbf{m} \times \mathbf{H}_{\text{eff}} - \alpha\gamma \mathbf{m} \times (\mathbf{m} \times \mathbf{H}_{\text{eff}}). \tag{10}$$

Equation eq:LLG preserves $|\mathbf{m}| = 1$ by construction.

2.3 Spin-Transfer and Spin-Orbit Torques

Current-driven dynamics can be modeled by adding torque terms to the righthand side:

• Slonczewski-like spin-transfer torque (STT) for spin-polarized current:

$$\mathbf{T}_{\text{STT}} = -(\mathbf{u} \cdot \nabla)\mathbf{m} + \beta\, \mathbf{m} \times (\mathbf{u} \cdot \nabla)\mathbf{m},$$

where $\mathbf{u} \propto Pj/(eM_s)$ is proportional to current density j and spin polarization P. • Spin-orbit torque (SOT) phenomenology includes damping-like and fieldlike terms:

$$\mathbf{T}_{\mathrm{SOT}} = \tau_{\mathrm{DL}}\,\mathbf{m} \times (\mathbf{m} \times \hat{\sigma}) + \tau_{\mathrm{FL}}\,\mathbf{m} \times \hat{\sigma},$$

where $\hat{\sigma}$ is the spin-polarization direction due to spin Hall or Rashba effects.

3 Numerical Methods

Direct analytical solutions of LLG are possible only in highly idealized geometries. Numerical simulation is therefore central. Two principal spatial discretization strategies are widely used: finite difference (FD) on regular grids and finite element (FE) on unstructured meshes.

3.1 Spatial Discretization

Finite difference method FD discretizes the magnetic body into cubic or rectangular cells. Spatial derivatives for exchange are approximated by central finite differences. The magnetostatic field is efficiently computed via convolution with the demagnetizing tensor, often using fast Fourier transforms (FFT) under periodic or open boundary approximations. FD is well-suited to GPU acceleration (e.g., Mumax3) because of regular memory access patterns.

Finite element method FE handles complex geometries and non-uniform meshes better. It solves magnetostatics via boundary-element method (BEM) coupling or by solving Poisson problems with appropriate boundary conditions. FE can reduce numerical artifacts at curved boundaries and allows adaptive mesh refinement near domain walls or other localized features.

3.2 Time Integration

Time-stepping of the stiff LLG is a major numerical challenge. Common schemes include:

- Explicit Runge–Kutta (RK) methods (e.g., RK4) — simple but step-size limited by stiffness (exchange and small cell sizes).
- Heun / midpoint schemes — second-order accurate and used in many packages.
- Semi-implicit or implicit midpoint methods — allow larger step sizes, preserve magnetization norm (with projection), and improve stability. • Adaptive step methods (embedded Runge–Kutta-Fehlberg) — adjust step size based on error estimates.

An often-used algorithmic approach is to treat the precession term explicitly and the damping term implicitly (or use geometric integrators that preserve $|\mathbf{m}|$ exactly). Selecting the appropriate integrator is a trade-off between accuracy and computational cost.

3.3 Magnetostatics solution

Computing $\mathbf{H}_d$ is the most computationally expensive part for large systems:

- Convolution via FFT (FD-grid): $O(N \log N)$ complexity.
- Hybrid FE-BEM or hierarchical matrix methods for FE: more complex but efficient for large-scale, irregular geometries.
- Multigrid and fast multipole methods (FMM) can accelerate long-range interactions.

3.4 Boundary conditions and discretization errors

Boundary conditions (open, periodic) influence domain patterns due to stray fields. Numerical parameters (cell size, time step) must respect physical length/time scales: the cell size should be significantly smaller than the exchange length

$$\ell_{\mathrm{ex}} = \sqrt{\frac{2A}{\mu_0 M_s^2}},$$

to resolve domain walls accurately. Convergence studies (cell-size halving, energy convergence) are recommended for each study.

4 Micromagnetic Simulation Tools

Several mature simulation packages are widely used:

4.1 OOMMF

OOMMF (Object Oriented MicroMagnetic Framework) from NIST is a FDbased, extensible package with a long history. It uses standard integrators, supports scripting, and is a reference implementation for many algorithms.

4.2 Mumax3

Mumax3 is a GPU-accelerated FD solver designed for high performance on regular grids. It supports STT, SOT, DMI, and thermal fluctuations, and is widely used for large-scale simulations.

4.3 Finite-element packages

Nmag, Fidimag, and commercial multiphysics packages (e.g., COMSOL with magnetic modules) provide FE capability; they are suitable for complex geometry and coupled multiphysics problems (e.g., magnetoelastic coupling).

4.4 Comparison

FD/GPU (Mumax3) is best for large, regular problems requiring speed; FE is preferred for irregular shapes and precise boundary representation. OOMMF remains a stable, well-documented choice for smaller or benchmarking tasks.

5 Representative Case Studies

This section presents three canonical micromagnetic problems illustrating modeling choices and typical results. For each case, we give the geometry, material parameters, numerical settings, and expected results. Placeholder figures are included.

5.1 Case 1: Domain-wall dynamics in a nanostrip

Geometry and parameters Consider a Permalloy ($Ni_{80}Fe_{20}$)-like strip of length $L = 2$, width $w = 100$, and thickness $t = 10$. Typical parameters: $M_s = 8e5 A/m$, $A = 1.3e-11 J/m$, $\alpha = 0.01$. Cell size $\approx 2.5 \times 2.5 \times 10$.

Driving mechanism Apply a spin-polarized current along the strip producing STT with spin polarization $P = 0.4$ and current density $j = 1e12 A/m^2$, or apply an external in-plane magnetic field pulse.

Observables Measure domain wall velocity vs. current density or field; observe Walker breakdown and precessional regimes. Typical results show linear velocity increase up to Walker limit followed by oscillatory dynamics.

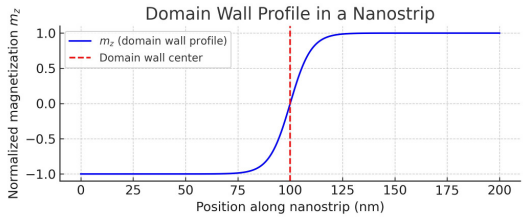

Figure 1: (Placeholder) Domain wall propagation in a nanostrip. Replace with simulation snapshots at successive times.

5.2 Case 2: Skyrmion stability and current-driven motion

Geometry and parameters Thin film (bilayer) geometry supporting interfacial DMI, with parameters: $M_s = 5e5A/m$, $A = 1e-11J/m$, $D = 3e-3J/m^2$, $\alpha = 0.03$, perpendicular anisotropy $K_u = 5e5J/m^3$. Use a 512×512 grid with lateral cell 1 for high resolution of skyrmion core.

Observables Compute skyrmion energy vs. radius, critical current for motion, skyrmion Hall angle (transverse deflection) under SOT. Investigate pinning at defects and thermal stability (Arrhenius behavior of lifetime with temperature).

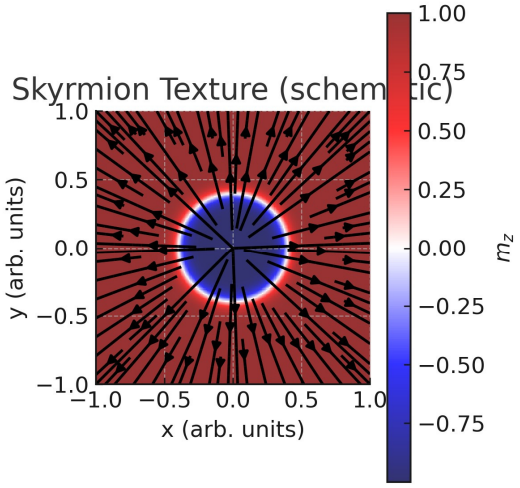

Figure 2: (Placeholder) Skyrmion texture in a thin film; color indicates m_z component.

5.3 Case 3: Magnetization reversal in nanoparticles (hysteresis)

Geometry and parameters An ensemble of single-domain ellipsoidal nanoparticles, or a patterned array, studied to extract hysteresis loops, coercivity, and switching field distributions. Simulations must include thermal fluctuations (stochastic LLG) when modeling temperature-dependent switching.

Observables Extract hysteresis curves, switching field distribution, coercivity vs. particle size and shape anisotropy. For thermal effects, use the Langevin thermal field:

$$\langle H_{\mathrm{th},i}(t) H_{\mathrm{th},j}(t') \rangle = \frac{2\alpha k_B T}{\gamma \mu_0 M_s V} \delta_{ij} \delta(t - t'),$$

where V is cell volume, k_B Boltzmann constant, and T temperature.

6 Recent Advances

6.1 GPU and HPC acceleration

The adoption of GPUs has transformed achievable simulation sizes and speeds. Efficient GPU implementations exploit data locality of FD grids and GPU FFT libraries. Multi-GPU and cluster-scale runs enable large-scale micromagnetic simulations spanning millions of cells.

6.2 Multiscale and hybrid methods

Bridging from atomistic spin dynamics to micromagnetics remains an active area. Hybrid schemes couple atomistic regions (where atomic-scale effects like non-collinearity are essential) to continuum regions treated by micromagnetics. Challenges include consistent transfer of exchange and spin currents across interfaces.

6.3 Machine learning in micromagnetics

Machine learning (ML) assists in surrogate modeling (fast approximations of hysteresis loops), parameter inference (learning material parameters from experimental images), and accelerating solvers by providing initial guesses or coarsegrained closures. ML models must respect physical invariances (rotation, gauge) for robust deployment.

6.4 Topological textures and spin-orbitronics

Interest in magnetic skyrmions, antiskyrmions, bimerons, and chiral domain walls has increased. Accurate micromagnetic modeling of these objects requires inclusion of DMI, temperature, and detailed materials parameters derived from experiments or ab initio calculations.

7 Validation, Benchmarking, and Best Practices

Benchmarking against analytical solutions (e.g., Walker breakdown velocity, Bloch wall width estimates) and cross-verification between codes (OOMMF vs. Mumax3 vs. FE codes) are essential. Report numerical parameters: cell size, time integrator, boundary conditions, and convergence tests. Use nondimensionalization where useful to compare across systems.

8 Challenges and Future Directions

- **Computational cost:** Long-range magnetostatics and fine meshes lead to heavy computation. Continued algorithmic improvements (FMM, hierarchical matrices, multigrid) and hardware advances are critical.
- **Multiphysics coupling:** Coupling magnetization dynamics with thermal transport, mechanics (magnetostriction), and electronic transport in a self-consistent manner remains challenging.
- **Parameter uncertainty and materials modeling:** Accurate input parameters (e.g., DMI strength, anisotropy) often require experiments or first-principles calculations; uncertainties propagate to simulation predictions.

- **Bridging scales:** Seamless coupling between atomistic spin models and micromagnetics to capture nucleation and interface phenomena is an active research area.
- **Reproducibility and data sharing:** Promoting reproducible simulation workflows and sharing datasets/benchmarks improves reliability and accelerates progress.

9 Conclusion

Micromagnetic simulation is a mature but rapidly evolving field, indispensable for understanding nanoscale magnetism and designing spintronic devices. Advances in algorithms, GPU computing, and multiscale coupling broaden the accessible problem space, while machine learning offers promising acceleration and inverse modeling tools. Future progress will increasingly depend on validated multiscale workflows, robust software engineering, and close integration with experiment.

Acknowledgments

Special thanks to Dr. Senoy Thomas for his valuable guidance.

A Numerical Implementation Details (Appendix)

A.1 Discretization of exchange

For a cubic FD cell with spacing h, the discrete Laplacian for the x-component m_x at cell (i,j,k) is

$$\nabla^2 m_x \approx \frac{m_{x,i+1,j,k} - 2m_{x,i,j,k} + m_{x,i-1,j,k}}{h^2} + (y, zterms).$$

The discrete exchange field is $\mathbf{H}_{\text{ex}} = \frac{2A}{\mu_0 M_s}\nabla^2 \mathbf{m}$.

A.2 Time step selection

For explicit RK methods, a heuristic time-step limit is

$$\Delta t \frac{\ell_{\text{ex}}^2}{2\gamma A} \approx C \frac{\mu_0 M_s}{\gamma} \left(\frac{h}{\ell_{\text{ex}}}\right)^2,$$

and it must be reduced as cell size h decreases. Implicit/semi-implicit schemes relax this constraint.

References

[1] W. F. Brown, Jr., "Micromagnetics," *John Wiley & Sons*, 1963.

[2] A. Aharoni, *Introduction to the Theory of Ferromagnetism*, 2nd ed., Oxford Univ. Press, 1996.

[3] L. D. Landau and E. M. Lifshitz, "On the theory of the dispersion of magnetic permeability in ferromagnetic bodies," *Phys. Z. Sowjet.*, 1935.

[4] T. L. Gilbert, "A phenomenological theory of damping in ferromagnetic materials," *IEEE Trans. Magn.*, 2004.

[5] J. C. Slonczewski, "Current-driven excitation of magnetic multilayers," *J. Magn. Magn. Mater.*, 1996.

[6] A. Thiaville, S. Rohart, E. Ju´e, V. Cros, and A. Fert, "Dynamics of´ Dzyaloshinskii domain walls in ultrathin magnetic films," *EPL*, 2012.

[7] A. Hubert and R. Sch¨afer, *Magnetic Domains: The Analysis of Magnetic Microstructures*, Springer, 1998.

[8] M. J. Donahue and D. G. Porter, "OOMMF User's Guide, Version 1.0," National Institute of Standards and Technology, 1999.

[9] A. Vansteenkiste et al., "The design and verification of Mumax3," *AIP Advances*, 2014.

[10] R. W. Chantrell et al., "Nmag: Finite element micromagnetic simulator," user docs.

[11] N. Nagaosa and Y. Tokura, "Topological properties and dynamics of magnetic skyrmions," *Nature Nanotechnology*, 2013.

[12] S. Zhang and Z. Li, "Roles of nonequilibrium conduction electrons on the magnetization dynamics of ferromagnets," *Phys. Rev. Lett.*, 2004.

[13] W. F. Brown, "Thermal fluctuations of a single-domain particle," *Phys. Rev.*, 1979.

[14] A. Barros et al., "Multiscale modelling of magnetic nanostructures: coupling atomistics and micromagnetics," *J. Phys.: Condens. Matter*, 2019.

[15] H. Fangohr et al., "Fidimag: software for micromagnetic simulations," user docs.

[16] G. Bertotti, *Hysteresis in Magnetism*, Academic Press, 1998.

[17] I. Dzyaloshinsky, "A thermodynamic theory of 'weak' ferromagnetism of antiferromagnetics," *J. Phys. Chem. Solids*, 1958.

[18] A. P. Malozemoff and J. C. Slonczewski, *Magnetic Domain Walls in Bubble Materials*, Academic Press, 1979.

[19] Y. Wang et al., "Machine learning for micromagnetics: a review," *Computational Materials Science*, 2020.

